Estimation of the divergence characteristics of a jet transport aircraft wing using numerical method.

Kirubeil Awoke Ferede (kb1981gc@gmail.com)
University of Gondar School of Technology

Research Article

Keywords: Aeroelasticity, Wing divergence speed, Aerodynamics Strip theory, Torsional influence coefficient, Numerical Method, Matrix iteration,

Posted Date: February 10th, 2022

DOI: https://doi.org/10.21203/rs.3.rs-1317086/v1

Estimation of the divergence characteristics of a jet transport aircraft wing using numerical method.

Kirubeil Awoke Ferede

Department of Mechanical Engineering, University of Gondar, Technology Institute, Gondar Ethiopia.
Postal dress:197, Phone: +251922956733
E-mail: kiru1981gc@gmail.com

KEYWORDS

Aeroelasticity
Wing divergence speed
Aerodynamics Strip theory
Torsional influence coefficient
Numerical Method
Matrix iteration

ABSTRACT

The goal of the present paper work is to demonstrate the use of numerical matrix iteration technique to obtain the divergence speed of a jet transport aircraft wing by employing aerodynamic strip theory. Aerodynamics strip theory is employed to obtain the divergence speeds for a finite (Three Dimensional) wing and for an infinite (Two dimensional) wing by matrix iteration technique. The aircraft wing is divided in to a number of Multhopp's stations. The elastic property of the wing of a typical jet transport is considered for this analysis. Assuming a straight elastic axis, the matrix of torsional influence coefficients associated with Multhopp's stations has been computed. A MATLAB code is used to iterate the matrix to arrive at the required convergent approximate solution. The solution converges about after ten iterations of the matrix. It is observed that torsional divergence speed estimated on the basis of strip theory without finite span correction is about 18% lower than the divergence speed estimated on the basis of strip theory with finite span correction. Two-dimensional torsional divergence analysis based on strip theory yields conservative torsional divergence speed. A tentative increase of 20 % in torsional stiffness resulted in about 15.5 percent increase in torsional divergence speed of a three-dimensional wing. This shows that divergence speed of a wing is directly proportional to the square root of torsional stiffness. This corroborates the result obtained for a two-dimensional wing. The result of the findings will be mandatory to high performance modern airplane designers for aeroelastic analysis.

1. Introduction

Aero-elasticity is a multidisciplinary science which studies the mutual interaction among aerodynamic, inertia, and elastic forces and the influence of these interaction upon airplane design. No aircraft structure is completely rigid, so when it is subjected to aerodynamic forces it will normally deflect by a small amount [1]. This effect can become very important at high speeds because any change in the shape of the body can cause the applied aerodynamic forces to change, leading in turn to further deflection and further changes in load. This vicious circle can rapidly develop in to aero-elastic phenomena. The flexibility of modern airplane structure is responsible for various aero-elastic problems. The various aero-elastic phenomena are classified in to static aeroelastic phenomena and dynamic aeroelastic phenomena. Dynamic aeroelasticity involves the interaction among aerodynamic, elastic and inertia forces and include problems like flutter, buffeting, dynamic response, gust load, life cycle oscillations and so on [2,3]. On the other hand, static aeroelastic problem involve the interaction between aerodynamic and elastic forces. These problems include control surface reversal (aileron, elevator), divergence (wing, tail plane), control effectiveness, load distribution and aeroelastic effects on static stability.

A serious of research in aeroelasticity started during the development of cantilever monoplane aircraft. The aeroelastic problems in the early days of monoplane design were overcome by cut-and-try method [4,5]. A theory of wing load distribution and wing divergence presented by [6-9]. A theory of lateral loss of lateral control and aileron reversal was latter published by [10]. More recent development in the wing aeroelastic problem related to techniques for casting the equations of equilibrium in matrix form. Such techniques are useful in the treatment of wings with non-uniform properties. Moreover, [11] and [12] have provided the basis for application of matrices to straight wing aeroelastic problems. Design of high-speed aircraft is considerably influenced by flutter. Modern aircrafts are subjected to many kinds of flutter phenomena like classical flutter and stall flutter. Flutter consideration controls wing skin thickness, wing platform and aspect ratio. Decreasing in wing aspect ratio and increasing in sweep tend to raise flutter speed. Heavy mass items in the wing are often located by consideration of optimum conditions for flutter prevention [4,13]. Another most common aeroelastic problem is wing torsional divergence of a straight wing. Design parameters affecting divergence of a straight wings are primarily wing torsional stiffness and offset distance between center of twist and aerodynamic center. Raising the divergence of a wing by increasing torsional stiffness is a costly process at the expense of considerable weight. An approach more frequently employed by designers is to proportion

47 the wing structurally so as to move the center of twist forward and thus reduce the aerodynamic eccentricity. For
48 example, a straight wing, which carries its torsional load by a D-box has a forward center of twist location and
49 subsequently a high divergence [4,14].

50 The main aim of this research article is to demonstrate the use of numerical matrix iteration technique to
51 characterize the divergence speed of a jet transport aircraft wing by employing aerodynamic strip theory.

52 Phenomena of wing divergence is a primary interest to the airplane structural designer. Divergence speed
53 of sweptback wings is inherently high. However, divergence speed of swept forward wings is so low that for this
54 reason alone, swept forward is practically ruled out as a design feature [15]. A plethora of research paper has been
55 published by various researchers on aeroelastic phenomena, particularly on flutter and wing divergence. Research
56 reported by [16] investigated the influence of the stiffness on the flutter characteristics of High aspect ratio wing. In
57 their study, they employed fluid structure coupling method to examine the flutter phenomena of the wing. The
58 corotational (CR) method was carry out for structural analysis. The loads were analyzed based on the result obtained
59 from computational fluid dynamics (CFD) solver. The results show that, for a wing span wise direction increase of
60 bending stiffness and torsional stiffness, there is a significant reduction of flutter amplitude as compared with the
61 original wing. Another researcher group analyzed the influence of wing linear or quadratic pretwist distributions, and
62 the effect of various twist angles on the aeroelastic stability an aircraft. The researchers modeled the wing structure as
63 beam theory of Hodges. The study revealed that by pretwisting the wing, flutter speed of the wing with respect to the
64 untwist wing increases until a specific twist value and then decreases. Moreover, adding the pretwist to the wing
65 decreases the flutter frequency. The obtained findings were compared with those reported in the literature and excellent
66 agreement has been noted [17]. The influence of delamination on the flutter and divergence character of a composite
67 wing using exact methods was investigated. The study of this paper assumed the wing frame as a cantilevered
68 Bernoulli–Euler beam with coupled bending–torsion and delaminated wing panel assumed as three interconnected
69 integral beams. The finding of the study has shown that the effect of fiber angle on the local delamination and its
70 length has an influence on the flutter behavior of the wing [18]. An indirect way of studying flutter and divergence
71 responses as a design constraint with the object of weight optimization was assessed [19]. The researchers applied the
72 level set method for their wing topology optimization computation. The result of the study provided insights into
73 optimal aeroelastic design of innovative aircraft structural configurations. The static aeroelastic instability mainly

wing torsion divergence optimization of swept forward wing was reported by a group of researchers. This research group applied an aeroelastic tailoring technique-based radial basis function neural networks (RBFNNs) and genetic algorithm (GA) optimization in MATLAB on the bases of the material orientation, thickness, and lay-up as a design decision parameter through finite element method (FEM) structural analysis. According to the report, the torsional instability of forward swept wing increased at subsonic speeds and decreased at supersonic with the increase of flight velocity [20]. Using the finite element method, the effect of in-plane stresses and lamination parameter on the flutter or divergence instabilities for constant stiffness and variable stiffness of edge-supported and cantilever composite trapezoidal panels were investigated [21]. The researchers applied the first-order piston theory and eigenvalue analysis to assess aeroelastic instability of such a wing. With the employment of analytical approach, a further study on the aeroelastic behavior of a composite wing was examined [22]. The researchers analyzed thin-walled single-cell closed cross-section beam with circumferentially asymmetric stiffness (CAS) configuration. In their study, they estimated the best layup configuration fiber orientation angle for the maximum flutter speed. The result of the study revealed the benefits of foam filled model over the non-foam filled model in terms of the flutter speed to the weight ratio. For both the straight and swept-back wings, the influence of laminate pattern (composite layup) on the wing divergence and flutter behavior was investigated based on the coupling of Finite Element Model (FEM) with vortex lattice method and Finite Element Model (FEM) with doublet lattice method respectively [23]. In their investigation, they portion the plate wing structure into linear triangular elements with five degrees of freedom at each node. To evaluate the result with others published works, a MATLAB code was used. The result of the study showed that composite layup orientation angles have played a great role which can be considered as a design parameter for the aero elastic instability analysis of on the wing flutter and divergence speeds. Modified higher order shear deformation theory for the structural computation and Doublet point method for the aerodynamic unsteady flow formulations were applied for the aeroelastic instability analysis [24]. The researchers used U-g method for flutter and divergence velocities estimations. The findings showed that positive fiber angles produce divergence-free wings, but the flutter speeds were small relative to negative fiber angle wings, which resulted a challenge to achieve composite tailoring that at the same time realizes high-flutter and high-divergence boundaries. Poisson's integral equation was also involved in the static stability of a thin plate [25]. In the research report of this paper, the point at which the static instability of a plate wing that could be described by partial differential equations (PDE) are considered to be the divergence speeds which indicate static instabilities start to occur. With the application of the Hamilton's principle and finite element

formulation, Mengchun Yu and Chyanbin Hwu [26] characterized aeroelastic divergence an element wise full model tapered composite wings. It was observed that the divergence peed increased with increased in taper ratio of the wing. An indirect way of studying using numerical approach, the effect of structural sensitivity on the wing divergence and flutter speed behavior of a typical wing section, based Monte Carlo simulation was assessed by [27]. A further study by a team of researchers [28] used numerical and experimental support to address the aeroelastic behavior of a wing. The researchers selected AGARD 445.6 wing design for their numerical analysis and they coupled computational fluid dynamics and computational structural dynamics in the ANSYS environment. They also validated their findings with the experimental approach and hence they found an agreement with each other. Another group of researchers [29] used a higher-order shear deformation theory (HSDT) with higher-order finite element modeling (FEM) to study the divergence and flutter characteristics of composite plate wings. The researcher familiarized new higher-order composite plate element, titled MONNA, and coupled with the vortex lattice, doublet lattice, and doublet point aerodynamic panel method models to show the research approach. The research finding showed that the new plate element approach has a better divergence-flutter convergence and accuracy as compared to traditional elements. A further study using numerical methods in the divergence and flutter analysis of multilayered laminated structures was developed [30]. Panel methods such as Vortex-Lattice used to calculate the pressure distribution, Piston Theory used to for Flutter characteristics and Movchan-Krumhaar Methods were utilized to evaluate the structural stability when structural viscous damping is considered for the study. The researcher used commercial FE package such as DYNAMICS Module of NISA for their calculation. Structural parameters such as fiber orientations, stacking sequences and boundary condition and different flow angles were considered. Matrix iteration methods are usually the choice for many aero-structural and aeronautical engineers to analyze complex structures of flying vehicles because of their tool accessibility, flexibility and ability to solve complex problems [9]. In general, from the literature different approaches and attempts have been made to estimate the divergence characteristics of the wing of a jet transport aircraft in terms of critical divergence speed beyond which the catastrophic failure of the aircraft occurs. The goal of the present paper work is by employing strip theory [31−34], with finite span correction (3D) and without finite span correction (2D) fluid flow to demonstrate the use of matrix iteration technique to obtain the divergence speed of a jet transport aircraft wing. The strip theory of aerodynamics assumes the two-dimensional flow of fluid through the wing airfoil section. In the present paper, first the elastic properties of a straight wing in terms of wing torsional influence coefficients have been determined. Secondly, equilibrium equations are derived in the form of an

integral equation. Then, an appropriate choice of aerodynamic theory in the form of strip theory has been discussed and the method of solution for finding the divergence speed has been dealt. Finally, the integral equation has presented in matrix form using strip theory and observations on the governing equations has been made. A MATLAB code has been used to iterate the matrix to reach for the solution to converge.

2. Structural theory and analysis

Modern airplanes vary widely in geometric shape. On the other hand, we find high aspect ratio wings such as the Boeing-47 airplanes which resembles slender beam, and on the other hand, low aspect ratio delta wings such as Canvair XF-92 that resemble plates. The wings of jet transport aircraft, which is related to the present work resemble a beam structure and the analysis carried out in this work shall use beam equation. The object of this section is to discuss the method of analysis of deformation of a wing structure under static load, considering it to represent a beam and to determine torsional influence coefficients, which represents torsional rigidity of the wing structure [4].

2.1 Elastic properties of a wing structure.

It is assumed that the wing of the transport aircraft under consideration is perfectly elastic. That is when the external forces are removed, the wing structure resumes its original form. Experiments on aircraft structure have shown that within certain limits, the force and the deflection are linearly related. In the skin of aircraft wing structure elastic buckling may produce a discontinuity in the force deflection diagram even though the material that make up the wing structure are stressed at relatively low level. Therefore, the elastic behavior of the wing structure is defined in the range below the point of elastic buckling.

2.1.1 Concept of influence coefficients.

The concept of influence coefficients is applied in this analysis, where the wing structural deformation due to several forces and moments are considered [4,35]. Consider a general case shown in Fig 1. Based on this approach, the total linear and angular deflection of any point can be expressed as the sum of the deflections at that point produced by individual forces and moments. This is stated by the principle of superposition, which is the base for the analysis of linear system. In Fig 1, the symbol Q is assigned to the arbitrary force or moment called “generalized forces”. Similarly, the symbol q is assigned to the linear or angular displacement of the point of application of each generalized forces and is called “generalized coordinates”. Generalized coordinates are quantities, which represent the possible

independent displacement of the system. Hence, they must not violate the geometric constraints imposed up on the system. Such a constraint implies that wing deflection at the point of attachment to the fuselage must be zero.

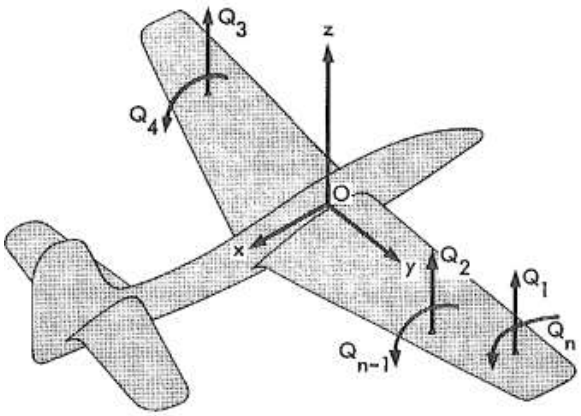

Fig. 1. Several discrete forces and moments applied to elastic structure [4].

By the principle of superposition, the displacement of the point of application of the i[th] generalized force due to n generalized forces is given by

$$q_i = \sum_{j=1}^{n} C_{ij} Q_j \qquad (i = 1,2,3, \ldots . n) \tag{1}$$

where the constants C_{ij} are called flexibility influence coefficients.

In matrix notation, the above equation can be expressed as:

$$\begin{bmatrix} q_1 \\ q_2 \\ . \\ . \\ . \\ q_n \end{bmatrix} = \begin{bmatrix} C_{11} & C_{12} & \cdot & \cdot & \cdot & C_{1n} \\ C_{21} & C_{22} & \cdot & \cdot & \cdot & C_{2n} \\ . & . & \cdot & \cdot & \cdot & . \\ . & . & \cdot & \cdot & \cdot & . \\ . & . & \cdot & \cdot & \cdot & . \\ C_{n1} & . & \cdot & \cdot & \cdot & C_{nn} \end{bmatrix} \begin{bmatrix} Q_1 \\ Q_2 \\ . \\ . \\ . \\ Q_n \end{bmatrix} \tag{2}$$

In short matrix notation, it can be expressed as: $\{q\} = [C]\{Q\}$. (3)

Influence coefficients and their matrices have the important property of symmetry. This property is expressed by: $C_{ij} = C_{ji}$ [35].

Consider the properties of the matrix [C], which apply to Fig 1. When n=4, it can be portioned in to four matrixes each containing different types of influence coefficients as follows:

$$[C] = \begin{bmatrix} C_{11}^{\delta\delta} & C_{12}^{\delta\delta} & C_{13}^{\delta\alpha} & C_{14}^{\delta\alpha} \\ C_{21}^{\delta\delta} & C_{22}^{\delta\delta} & C_{23}^{\delta\delta} & C_{11}^{\delta\delta} \\ C_{31}^{\alpha\delta} & C_{32}^{\delta\delta} & C_{33}^{\alpha\alpha} & C_{11}^{\delta\delta} \\ C_{41}^{\alpha\delta} & C_{42}^{\delta\delta} & C_{43}^{\delta\delta} & C_{44}^{\alpha\alpha} \end{bmatrix} \quad (4)$$

The four types of elements are:

$$C^{\delta\delta} = linear\ deflection\ at\ i\ due\ to\ unit\ force\ at\ j.$$

$$C^{\alpha\alpha} = linear\ deflection\ at\ i\ due\ to\ unit\ moment\ at\ j.$$

$$C^{\delta\alpha} = linear\ deflection\ at\ i\ due\ to\ unit\ force\ at\ j.$$

$$C^{\alpha\delta} = linear\ deflection\ at\ i\ due\ to\ unit\ moment\ at\ j.$$

For the matrix [C] to be symmetrical, the reciprocal theorem of Betti [33] must hold:

$$C_{ij}^{\delta\delta} = C_{ji}^{\delta\delta}, C_{ij}^{\alpha\alpha} = C_{ji}^{\alpha\alpha}, C_{ij}^{\delta\alpha} = C_{ji}^{\alpha\delta}$$

2.1.2 Expression of strain energy based on influence coefficients

In the application of energy theorem to aeroelastic system, formulas for strain energy in terms of influence coefficient, referring to Fig 1, can be defined as:

$$U = \frac{1}{2}\sum_{i=1}^{n} Q_i q_i. \quad (5)$$

Substituting equation (1) in to equation (5), gives the expression of strain energy in terms of flexibility influence coefficients:

$$U = \frac{1}{2}\sum_{i=1}^{n}\sum_{j=1}^{n} C_{ij} Q_i Q_j. \quad (6)$$

In order to express the strain energy in integral form, consider a wing section shown in the Fig 2. A point on the cross section is located by the wing span wise coordinate y and the tangential coordinate s. the tangential coordinate is measured positive in the counter clock wise direction for the peripheral skin and is positive in the positive direction of the Z-axis for the interior webs.

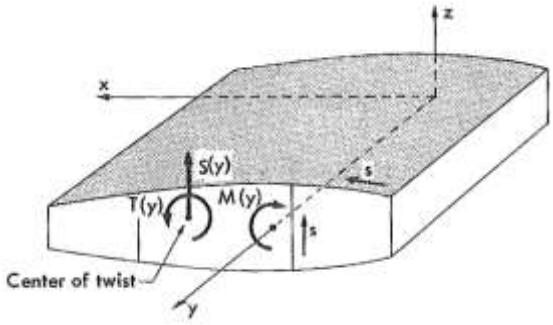

Fig. 2. Loaded cross section of shell beam [4].

A loaded cross section at a distance y from the origin is acted up on by a torque T(y) with positive direction as shown in Fig 2. The point of application of T(y) is at the center of twist or shear center of the section. Shear flow assumes positive in the S-direction and denoted by q.

If, during the application of twisting moments, the beam is free to warp, the strain energy is due entirely to shear stress and given by:

$$U = \frac{1}{2G}\int_0^l \int_{c.s} q^2 \frac{ds}{t} d\lambda \tag{7}$$

Application of Castigliano's theorem, to the equation (7) gives the angle of twist of the beam due to the given distributed applied torque T(y) as follows:

$$\theta(y) = \frac{\partial U}{\partial T} = \frac{1}{G}\int_0^l \int_{c.s} q(\lambda, s) \frac{\partial q}{\partial T} \frac{ds}{t} d\lambda \tag{8}$$

where $q(\lambda, s) = shear\ flow\ distribution\ due\ to\ applied\ torques$;

$\frac{\partial q}{\partial T} = shear\ flow\ distribution\ due\ to\ unit\ torque$;

$T = 1\ applied\ at\ the\ spanwise\ section$;

If we now assume that the shear flow distribution due to T=1 is denoted by $\vartheta(\lambda, s), then$

$$q(\lambda, s) = T(\lambda)\vartheta(\lambda, s)$$

$$\frac{\partial q}{\partial T} = \begin{cases} \vartheta(\lambda, s) & (y > \lambda) \\ 0 & (y < \lambda) \end{cases} \tag{9}$$

Substituting equation (9) in to equation (8), we have

$$\theta(y) = \int_0^y \frac{T(\lambda)d\lambda}{GJ} \tag{10}$$

where $J = \frac{1}{\int_{c.s} \vartheta^2 \frac{ds}{t}}$ is the torsional rigidity of the beam cross section. And the quantity GJ is called the torsional stiffness of the beam.

Differentiating equation (10) with respect to y, we get a relation between the applied torsional moment and rate of twist as follows:

$$\frac{d\theta(y)}{dy} = \theta' = \frac{T}{GJ} \tag{11}$$

2.2 Torsional influence coefficients

Consider a cantilever wing subjected to unit torque load as shown in the Fig. 3 below. A unit torque about the elastic axis is applied at a distance η from the origin and the resulting angular displacement at y is denoted by $C^{\theta\theta}(y, \eta)$.

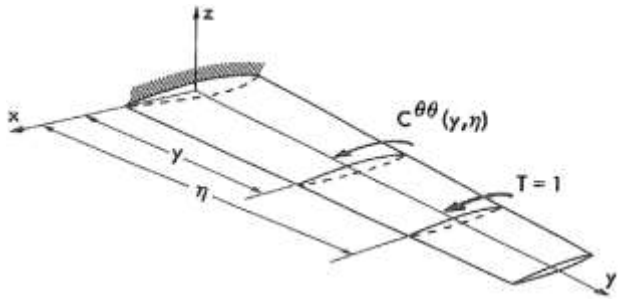

Fig. 3. Cantilever wing under unit torque load [4].

As defined earlier,

$$q(\lambda, s) = \vartheta(\lambda, s) \ldots\ldots\ldots\ldots\ldots\ldots (0 < \lambda < \eta) \tag{12}$$

$$\frac{\partial q}{\partial T} = \vartheta(\lambda, s) \ldots\ldots\ldots\ldots\ldots\ldots (0 < \lambda < y) \tag{13}$$

Thus for $\eta > y$

$$C^{\theta\theta}(y, \eta) = \int_0^y \frac{d\lambda}{GJ} \tag{14}$$

And for $\eta < y$

$$C^{\theta\theta}(y,\eta) = \int_0^{\lambda} \frac{d\lambda}{GJ} \tag{15}$$

The torsional constant J, defined in equations (14) and (15) can be evaluated at each section of the beam, if the shear flow distribution $\vartheta(s,\lambda)$ due to a unit torque is known. This requires knowledge of the wing skin thickness, flange, web and stringer thickness etc at each section of the wing, in addition to the values of shear modulus at each section. The curve of torsional rigidity GJ has been computed in ref [4] and plotted in in Fig. 4.

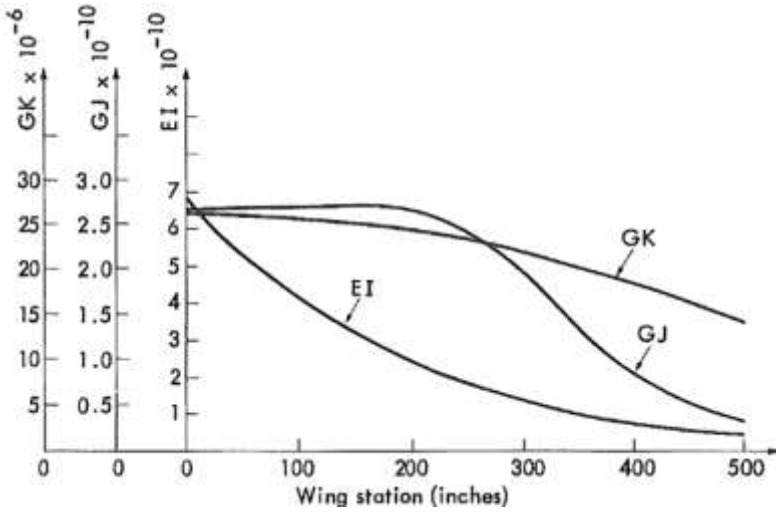

Fig. 4. (a) Bending, torsional, and shear stiffness curves.

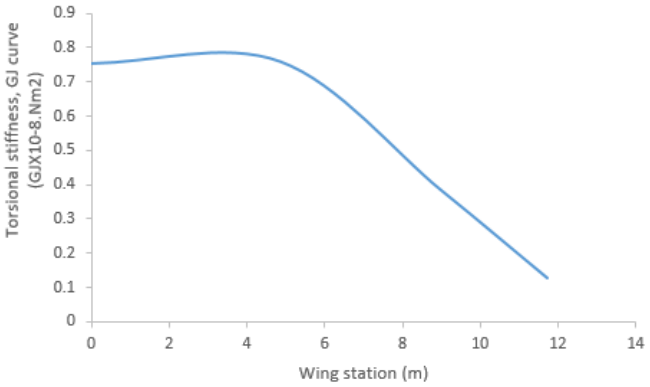

Fig. 4. (b) Torsional stiffness curve (changed to SI unit)

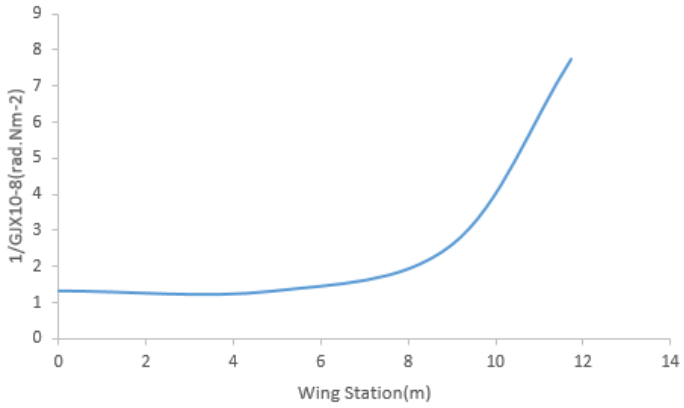

Fig. 4. (c) 1/GJ curve (changed to SI unit)

2.2.1 Geometric and elastic data of a jet transport aircraft wing

Here the elastic axis is straight and perpendicular to the root at 35% of the chord. The torsional rigidity GJ and the corresponding torsional flexibility 1/GJ have been computed at each section from the torsional rigidity curve in Fig. 4 (b) and are given below:

Table 1 Wing torsional stiffness values at the various Multhopp's stations [4]

Wing station (m)	$GJ \times 10^{-8}(Nm^2)$	$\frac{1}{GJ \times 10^{-8}}(rad.Nm^{-2})$
0	0.7553	1.324
4.86	0.7610	1.314
8.98	0.3874	2.581
11.73	0.1293	7.736

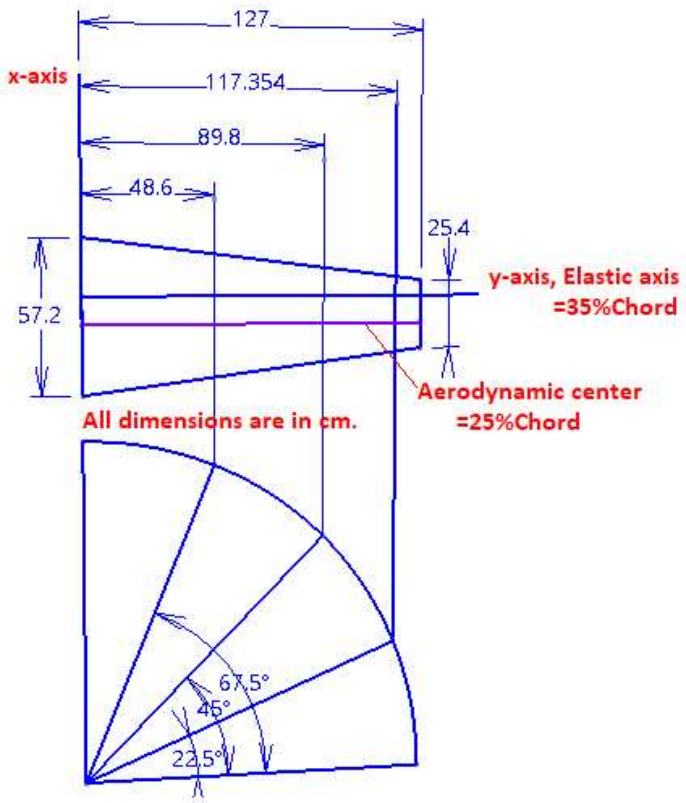

Fig. 5. Multhopp's stations [4,36]

2.2.2 Numerical evaluation of torsional influence coefficients Matrix

A plot of 1/GJ curve, as computed by the values of GJ at a number of sections along the span is shown in Fig. 4 (c) the wing is divided in to four stations over the semi-span as illustrated in Fig. 5. These particular stations called Multhopp's stations are selected for convenience in computing the aerodynamic matrixes. These stations are found to be a distance of 0, 4.86, 8.98 and 11.73 from the root in meters. For this work, the assumed wing stations are four, the resulting torsional coefficients matrix $[C^{\theta\theta}]$ is a (4x4) square matrix as shown below.

$$[C^{\theta\theta}] = \begin{bmatrix} C_{11} & C_{12} & C_{13} & C_{14} \\ C_{21} & C_{22} & C_{23} & C_{24} \\ C_{31} & C_{32} & C_{33} & C_{34} \\ C_{41} & C_{42} & C_{43} & C_{44} \end{bmatrix}$$

The values of torsional influence coefficients are obtained from eq (14) and eq (15) by calculating the areas under the 1/GJ curve shown in Fig. 4 (c).

Therefore,

$$C_{11} = C_{12} = C_{13} = \int_0^{11.73} \frac{d\lambda}{GJ} = 37.53 \times 10^{-8}\ rad.N.m^{-1}$$

$$C_{22} = C_{23} = \int_0^{8.98} \frac{d\lambda}{GJ} = 14.48 \times 10^{-8}\ rad.N.m^{-1}$$

$$C_{33} = \int_0^{4.86} \frac{d\lambda}{GJ} = 6.435 \times 10^{-8}\ rad.N.m^{-1}$$

The resulting matrix of torsional influence coefficient will be:

$$[C^{\theta\theta}] = \begin{bmatrix} 37.53 & 37.53 & 37.53 & 0 \\ 37.53 & 14.48 & 14.48 & 0 \\ 37.53 & 14.48 & 6.435 & 0 \\ 0 & 0 & 0 & 0 \end{bmatrix} \times 10^{-8}\ rad.N.m^{-1} \quad (16)$$

3. Divergence analysis

Divergence, which is a static instability phenomenon, involves the interaction between the elastic and aerodynamic forces. Therefore, the divergence analysis requires the calculation of the steady aerodynamic coefficient matrix and the structural stiffness matrix. The present work focuses on the torsional divergence of a straight wing, which is the most common problem in aeroelasticity.

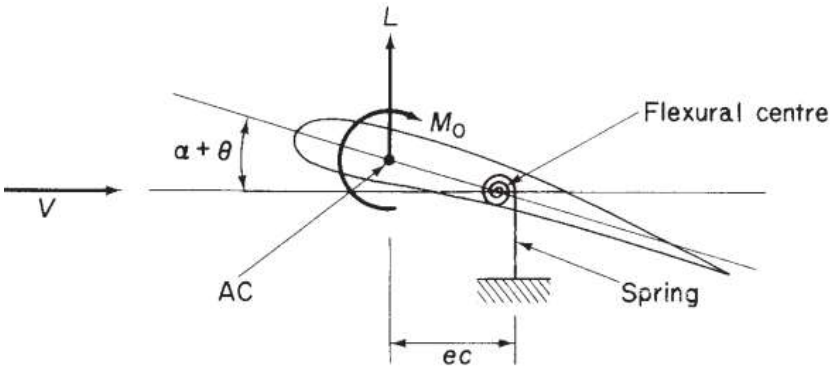

Fig. 6. Determination of wing divergence speed [33]

Consider the case of a simple straight wing at incidence (α) with center of twist behind the aerodynamic center. The pressure distribution with the main loads located near the nose is such as to cause the wing to twist in the nose up sense. Because the structure is not perfectly rigid, it gets in fact twisted, and its shape becomes distorted relative to the wing root section. It twists about an axis, known as the torsional axis or center of twist or flexural center of the

wing as shown in the fig 6 [33]. This twist, by increasing the effective incidence to (α+θ), creates a lift increment which then acts forward of the torsional axis, so that the effect is statically unstable, in the sense that the more it twists the bigger is the torsional moment tending to cause it to twist, of course, resisted by elastic forces due to twist still further. However, the tendency to twist is, of course, resisted by elastic forces due to the stiffness of the structure. This resistance to twist increases rapidly with the amount of twist, or strain, until it balances the aerodynamic twisting couple and equilibrium is reached. However, as the speed increases, the aerodynamic forces (L) increase rapidly, and therefore, so also does the twisting moment (Mo). The elastic stiffness is not affected by speed, and so the amount of twist increases with speed. Eventually, a speed is reached at which the elastic restoring torque is only just sufficient to counteract the twisting moment, and equilibrium is only reached with the wing breaking point. This speed is a critical speed called the wing torsional divergence speed. When this wing reached its torsional divergence speed, the increment in aerodynamic torsional moment due to an arbitrary increment in twist angle is exactly equal to the increment elastic restoring torque. When the speed exceeds the torsional divergence speed, the increment in aerodynamic torsional moment exceeds the increment in elastic restoring torque and the wing becomes statically unstable, and any increase in speed above this value will result in structural failure-the wing will break off.

3.1 Equilibrium equations

For the sake of simplicity, the following assumptions are made:

1. Straight wings are characterized by an elastic axis, which is perpendicular to the plane of symmetry of the airplane.
2. Chord wise segments of the wing remains rigid; that is, camber bending is negligible.

The differential equation of torsional aeroelastic equilibrium of a straight wing about its elastic axis is obtained by relating the rate of twist to applied torque as discussed earlier equation (11) is given as follows:

$$\frac{d\theta(y)}{dy} = \theta' = \frac{T}{GJ}$$

This can be rewritten as:

$$\frac{d}{dy}\left(GJ\frac{d\theta}{dy}\right) = \frac{dT}{dy} = -t(y) \tag{17}$$

where t(y)=applied torque per unit span

$\theta(y)$=elastic twist distribution.

Consider a slender straight wing subjected to aerodynamic and inertia forces as shown in Fig. 7.

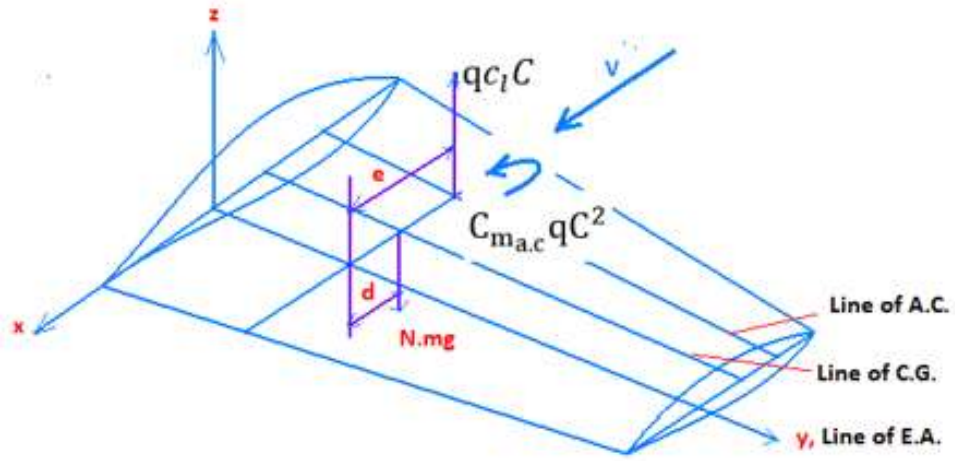

Fig. 7. Slender straight wing

Referring to Fig. 7, the applied torque per unit span t(y) is given by:

$$t(y) = qc_lce + qc^2C_{m_{ac}} - Nmgd \tag{18}$$

where $c_l = local\ lift\ coefficient$

$C_{m_{ac}} = local\ moment\ coefficients\ about\ the\ aircraft\ center$

$mg = wing\ weight\ per\ unit\ span$

$N = load\ factor\ normal\ to\ the\ wing\ surface$

$(N = 1\ for\ level\ flight)$.

Combining equation (17) and (18), we have the following differential equation of equilibrium as follows:

$$\frac{d}{dy}\left(GJ\frac{d\theta}{dy}\right) = Nmgd - qc_lce - qc^2C_{m_{ac}} \quad \text{or}$$

$$\frac{d}{dy}\left(GJ\frac{d\theta}{dy}\right) + qc_lce = Nmgd - qc^2C_{m_{ac}} \tag{19}$$

The boundary conditions are: $\theta(0) = 0;\ \theta'(l) = 0$.

The wing torsional deflection at any span wise location y due to torque t applied at span wise location η is derived from energy equation using Castiglione's theorem [4].

$$\theta(y) = \int_0^l C^{\theta\theta}(y,\eta)t(y)d\eta \tag{20}$$

Introducing equation (18) in to equation (20), we obtain:

$$\theta(y) = \int_0^l C^{\theta\theta}(y,\eta)\{[c_l ce + c^2 C_{m_{ac}}]q - Nmgd\}d\eta \tag{21}$$

We can regard the angle of attack as a superposition of a rigid angle and an elastic twist.

$$\alpha(y) = \alpha^r(y) + \theta(y) \tag{22}$$

Similarly, the local lift coefficient can be written as:

$$c_l(y) = c_l^r(y) + c_l^e(y) \tag{23}$$

Where $c_l(y) = local\ angle\ of\ attack\ measured\ from\ zero\ lift\ excluding\ elastic\ twist$

$$c_l^r(y) = local\ lift\ coefficient\ distribution\ resulting\ from\ rigid\ twist, \alpha^r(y)$$

$$c_l^e(y) = local\ lift\ coefficient\ distribution\ resulting\ from\ elastic\ twist\ .$$

Substituting equation (23) in to equation (19), we get the following integral equation:

$$\frac{d}{dy}\left(GJ\frac{d\theta}{dy}\right) + qcec_l^e = -qcec_l^r - qc^2 C_{m_{ac}} + Nmgd \tag{24}$$

Similarly, substituting equation (23) in to equation (21), we get the following integral equation:

$$\theta(y) = \int_0^l C^{\theta\theta}(y,\eta)ecc_l^e d\eta + \int_0^l C^{\theta\theta}(y,\eta)\left(ecc_l^r q + qc^2 C_{m_{ac}} - Nmgd\right)d\eta \tag{25}$$

$$\text{or} \qquad \theta(y) = q\int_0^l C^{\theta\theta}(y,\eta)ecc_l^e d\eta + f(y) \tag{26}$$

$$\textit{Where } f(y) = \int_0^l C^{\theta\theta}(y,\eta)\left(ecc_l^r q + qc^2 C_{m_{ac}} - Nmgd\right)d\eta.$$

Equation (26) is the required governing integral equation.

3.2 Strip theory Aerodynamic Formulation

Strip theory is one of the aerodynamic analysis tools which assumes flow along the wing section is two dimensional [2,31–34,37,38]. In Aerodynamic analysis the motion of the fluid can be framed as 2D problem for slender bod. Setting a given aerodynamic problem into 2D and applying strip theory it is noticed that there are much deviations in the crosswise direction as compared to that of longitudinal one. The principle behind the strip theory is that the portion of the wing submerged into the fluid flow is divided into finite number of strips and then 2D aerodynamic coefficients for added mass can be computed for each strip and then integrated over the length of the body to yield the 3D coefficients.

Referring to both $\theta(y)$ and $c_l^e(y)$ in equation (26), they are regarded as unknown functions and so the problem is mathematically indeterminate. The problem becomes mathematically determinate as soon as a second relation between the two unknowns is stated. This second relation is supplied by some appropriate choice of aerodynamic theory. The aerodynamic theory is assumed to involve a linear relation between angle of incident and lift distribution that can be represented by:

$$\alpha(y) = \Theta(cc_l) \tag{27}$$

where Θ = the linear operator on the lift distribution cc_l

to produce the required incidence distribution $\alpha(y)$.

Strip theory is defined as one in which Θ is simply, $\Theta = \frac{1}{a_0 c}$ (28)

where $a_0 = the\ local\ two\ dimentional\ slope\ of\ the\ lift\ coefficient\ curve.$

$c = the\ wing\ chord.$

4. Methods of solution by matrices using strip theory

Equation (26) together with equation (27) forms the basis for the prediction of elastic twist and lift distribution of an un-swept wing with the straight elastic axis.

The torsional divergence speed of a three-dimensional wing is determined from the lowest Eigen value of dynamic pressure q_d, determined from the integral equation of equilibrium in its homogenous form. The homogenous form of equation (24) is:

$$\frac{d}{dy}\left(GJ\frac{d\theta}{dy}\right) + q_d cec_l^e = 0 \tag{29}$$

The homogenous form of equation (26) is

$$\theta(y) = q_d \int_0^l C^{\theta\theta}(y,\eta) ecc_l^e d\eta \tag{30}$$

Equation (29) or (30) can be alternatively used together with equation (27) to compute the divergence speed.

It is usually necessary to employ numerical solution in practical airplane problems. In this case, the integral equation (30) with matrix methods possesses advantageous. Applying strip theory, equation (30) can be written as;

$$\frac{c_l^e}{\frac{dc_l}{d\alpha}} = q_d \int_0^l C^{\theta\theta}(y,\eta) ecc_l^e d\eta \tag{31}$$

Where $\frac{dc_l}{d\alpha}$ =the effective lift curve slope corrected for aspect ratio.

The matrix form of equation (31) can be written as follows:

$$[A]\{cc_l^e\} = q_d[E]\{cc_l^e\} \tag{32}$$

$$\text{where } [A] = \frac{1}{\frac{dc_l}{d\alpha}}\left[\frac{1}{C}\right]$$

$$E = \left[C^{\theta\theta}\right][e][\bar{W}] \tag{33}$$

$$\text{where } [\bar{W}] = wegting\ matrix.$$

Equation (32) is the governing equation in the matrix form for the numerical evaluation of divergence speed.

4.1 Observations

1. The torsional divergence speed of a three-dimensional wing is determined from the lowest eigenvalue of dynamic pressure q obtained from the homogenous differential equation (29) or integral equation of equilibrium equation (30).

2. Equation (29) or equation (30) can be alternatively used together with equation (27) to compute the divergence speed. They are both satisfied by the same infinite set of Eigen values and Eigen functions. The lowest Eigen value is the dynamic pressure q_d, corresponding to the torsional divergence. The corresponding Eigen function$\theta_d(y)$, is the span wise distribution at the divergence speed.
3. The integral equation form (equation (30)) serves as a convenient basis for numerical location of complex practical problems.
4. In both equations $\theta(y)$ and $c_l^e$are regarded as unknown function and hence the divergence problem is redundant with single degree of indeterminateness. The problem of redundancy is solved by additional equations (27) between the unknowns. Strip theory is employed to obtain this equation.
5. Solution to the differential equation (29) for the case of strip theory can be obtained in closed form in the case of cantilever wing of uniform chord and stiffness. However, we cannot obtain the solution in the closed form since the wing under consideration is both of varying chord and stiffness along the wing span.

5. Numerical solution and validation

The matrix form of the governing equation for the determination of the divergence speed of a jet transport wing has been developed and given by equation (32). This equation shall be used to estimate the divergence speed of a wing where torsional flexibility coefficient matrix $C^{\theta\theta}$ has been obtained numerically and is given by (16). The weighting matrix $[\bar{W}]$ is obtained by applying Multhopp's quadratic formula. The application of this formula is detailed in ref. [4] where it is shown that for a particular four station configuration that we have adopted in this work has the form of a diagonal matrix given by equation (36). The governing equations (32) is solved by matrix iteration technique using strip theory with or without finite span corrections.

5.1 Estimation of wing chord matrix

Since the wing considered is tapered, the chord varies along the wing span.

The wing root length, $C_0 = 225" = 5.715m$

The wing tip length, $C_t = 100" = 2.54m$

The span at any span length, y_i

The wing half span, $y = 22.86m$

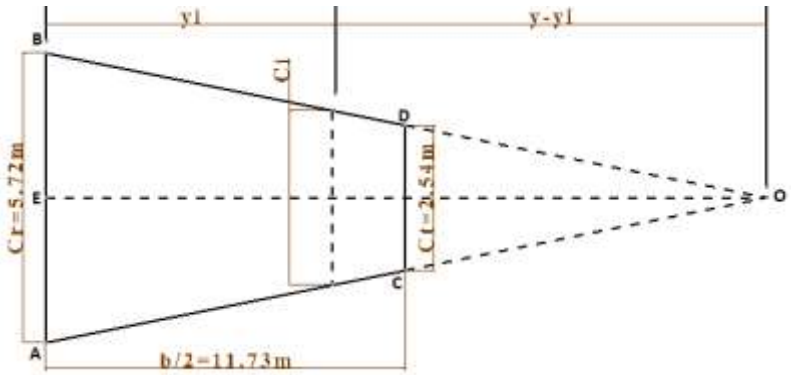

Fig. 8. Wing half span platform geometry [4].

From similarity of triangles, the chord length at any span length can be obtained by the following relations:

$$\frac{C_i}{C_t} = \frac{y - y_i}{y}$$

$$C_i = C_0\left(\frac{y-y_i}{y}\right) = C_0\left(1 - \frac{y_i}{y}\right) \tag{34}$$

Substituting the above numerical values will result in

$$C_i = 5.715\left(1 - \frac{y_i}{22.86}\right) \tag{34, a}$$

Computing the chord C_i at station 1, 2, 3, and 4; and putting the results in matrix form we will get the following diagonal matrix:

$$[C] = \begin{bmatrix} 2.78 & 0 & 0 & 0 \\ 0 & 3.48 & 0 & 0 \\ 0 & 0 & 4.5 & 0 \\ 0 & 0 & 0 & 5.715 \end{bmatrix}$$

5.2 Estimation of eccentricity

It is known that the location of wing aerodynamic center is quarter of the chord measured from the leading edge, i.e. $a.c = 0.25C$ and the elastic axis$= 0.35C$.

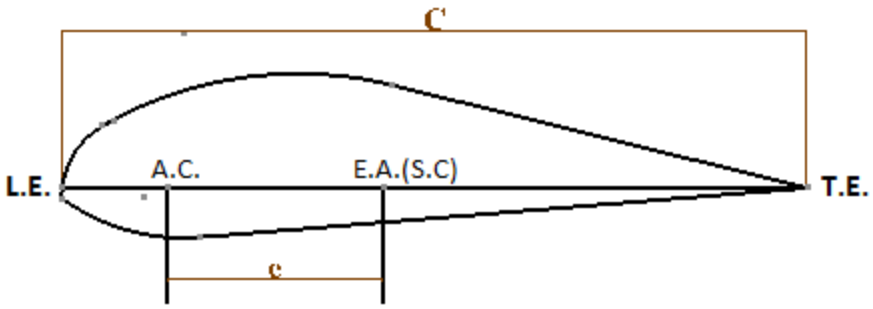

Fig. 9. Airfoil section showing aerodynamic and elastic axis (shear center).

The eccentricity e, the distance between the elastic axis and aerodynamic center, and is defined by e=0.35C-0.25C=0.1C. Since the chord c is variable or different for different sections, e also differs along the wing span.

Therefore, $$e_i = 0.1 \times C_i \tag{35}$$

The resulting diagonal eccentricity matrix is:

$$[e] = \begin{bmatrix} 0.278 & 0 & 0 & 0 \\ 0 & 0.348 & 0 & 0 \\ 0 & 0 & 0.45 & 0 \\ 0 & 0 & 0 & 0.572 \end{bmatrix}$$

5.3 Multhopp's quadratic formula

When functions arisen from lifting line theory, an approximate quadrature's developed by Multhopp's is convenient. For a symmetrical lift distribution problem, applying the methods and formula for a wing semi span $l = b/2$, we get the following diagonal matrix of weighting numbers [4,36].

$$[\bar{\mathbf{w}}] = \frac{\pi l}{8}\begin{bmatrix} \sin\frac{\pi}{8} & 0 & 0 & 0 \\ 0 & \sin\frac{\pi}{4} & 0 & 0 \\ 0 & 0 & \sin\frac{3\pi}{8} & 0 \\ 0 & 0 & 0 & \frac{1}{2}\sin\frac{\pi}{2} \end{bmatrix} \tag{36}$$

5.4 Estimation of wing divergence speed using strip theory without finite span correction.

From equation (33), that is $[E] = [C^{\theta\theta}][e][\bar{W}]$, and multiplying the corresponding matrix quantities, we get the following result.

$$[E] = \begin{bmatrix} 19.95 & 46.28 & 77.69 & 0 \\ 19.95 & 17.84 & 29.97 & 0 \\ 19.95 & 17.84 & 13.32 & 0 \\ 0 & 0 & 0 & 0 \end{bmatrix} \times 10^{-8} rad\, {}^{m}/_{N}$$

From equation (32), we get a simplified expression as follows:

$$\frac{1}{\frac{dc_l}{d\alpha}}\left[\frac{1}{C}\right] = q_d[E]$$

Rearranging the above expression, we get:

$$\frac{1}{\frac{dc_l}{d\alpha}} = q_d[C][E] \tag{37}$$

Now the product of the matrix [C] [E] becomes:

$$\begin{bmatrix} 0.554 & 1.285 & 2.160 & 0 \\ 0.693 & 0.621 & 1.043 & 0 \\ 0.897 & 0.803 & 0.599 & 0 \\ 0 & 0 & 0 & 0 \end{bmatrix} \times 10^{-6} \frac{rad \times m^2}{N}$$

```
%MATLAB script for iteration convergence
clc;
C=[37.53 37.53 37.53 0; 37.53 14.48 14.48 0; 37.53 14.48 6.435 0; 0 0 0 0]*0.00000001
e=[0.278 0 0 0; 0 0.348 0 0; 0 0 0.45 0; 0 0 0 0.572]
w=[1.91 0 0 0; 0 3.54 0 0; 0 0 4.6 0; 0 0 0 2.494]
E=C*e*w
c=[2.78 0 0 0; 0 3.48 0 0; 0 0 4.5 0; 0 0 0 5.715]
cE=c*E
A=c*E
clc;
A=[0.555  1.287  2.160  0; 0.694  0.621  1.043  0; 0.898  0.803  0.599  0; 0  0  0  0]*0.000001;
n=size(A,1)
tol=0.00001;
err=100;
x=[1 1 1 1]'
x=ones(n,1)
k=0;
while(err>tol)
x1=A*x;
[val,pos]=max(abs(x1));
eigen_val=x1(pos);
x2=x1/eigen_val;
err=max(abs(x2-x));
x=x2;
eigen_vec=x;
k=k+1;
end
fprintf('Break the loop when it converges after %d iterations', k);
```

After ten iterations, the matrix $[C][E] = 2.7717 \times 10^{-6} \frac{rad.m^2}{N}$. Substituting the dynamic pressure q_d by $\frac{1}{2}\rho v_{Dinf}^2$, $\rho = 1.225\ kg/m^3$ and $\frac{dc_l}{d\alpha}$=5.5, we get the divergence speed of $v_{Dinf} = 327.3\ {}^{m}/_{sec}$.

5.5 Estimation of divergence speed using strip theory with finite span correction.

The divergence speed of a finite wingspan, without finite span correction has been determined. In order to be practical and to estimate the divergence speed of practical wing, i.e., a finite wing, the strip theory corrected for finite span need to be considered; and computed as follow:

$$\frac{dc_l}{d\alpha} = a_0\left(\frac{AR}{AR+2}\right)$$, where $\left(\frac{AR}{AR+2}\right)$=finite span correction factor.

where $AR = \frac{b}{\bar{c}}$, =aspect ratio of wing flat form, where b=wing span, $\bar{c}$=geometric or standard mean chord.

As we can see in the above equation the aspect ratio changes with span of the wing. So, when the finite wing is considered, the effective lift coefficient curve slope $\frac{dc_l}{d\alpha}$ will be changes.

Now let's compute the aspect ratio: $AR = \frac{b}{\bar{c}}$. Since chord varies along the span, we need to calculate $\bar{c}$. But $\bar{c} = \frac{S}{b}$, where S=wing area.

For the present case the wing plan form looks the following.

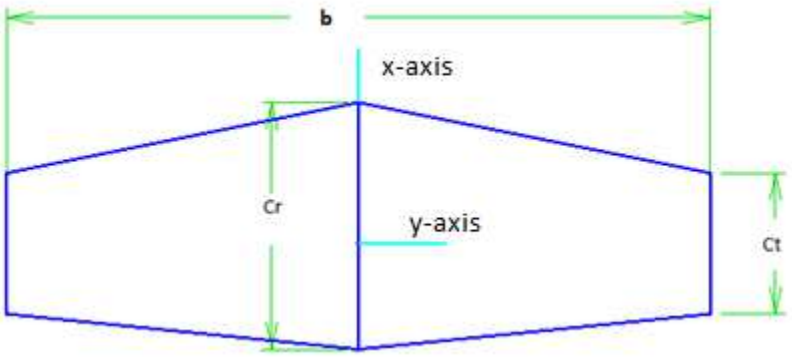

Fig. 10. Wing plan form

We know from equation (34, a) that$C_i = 5.715\left(1 - \frac{y_i}{22.86}\right)$

Substituting $\bar{c} = \frac{S}{b} = \frac{\int_{-b/2}^{b/2} C_i(y)dy}{\int_{-b/2}^{b/2} dy}$

Due to symmetry $\bar{c} = \frac{S}{b} = \frac{2\int_0^{b/2} C_i(y)dy}{b}$, where $b = \int_{-b/2}^{b/2} dy = 22.86m$

This implies $S = 2\int_0^{b/2} C_i(y)dy = 2\int_0^{12.7} 5.715(1 - \frac{y}{22.86})dy = 104.8385\, m^2$.

Therefore, $\bar{c} = \frac{S}{b} = \frac{104.8385}{22.86}$ =4.586m. $AR = \frac{b}{\bar{c}} = \frac{22.86}{4.586} = 5.0$

Therefore, the strip theory corrected for finite span:

$\frac{dc_l}{d\alpha} = a_0\left(\frac{AR}{AR+2}\right) = 5.5 \times \frac{5}{7}$ =3.93, where the constant $a_0 = 5.5$ is the lift slope

The divergence speed for the finite span correction becomes: $v_{Df} = 387.15m/sec$

5.6 Effect of increasing the stiffness rigidity, GJ of the wing on the speed divergence.

Let's assume 20% increment of GJ uniformly along the wing span. The resulting torsional flexibility influence coefficients matrix $[C^{\theta\theta}]$ becomes:

$$[C^{\theta\theta}] = \begin{bmatrix} 31.275 & 31.275 & 31.275 & 0 \\ 31.275 & 12.067 & 12.067 & 0 \\ 31.275 & 12.067 & 5.365 & 0 \\ 0 & 0 & 0 & 0 \end{bmatrix} \times 10^{-8} \frac{rad}{Nm^2}$$

The matrix product $[E] = [C^{\theta\theta}][e][\bar{W}] = \begin{bmatrix} 16.605 & 0 & 0 & 0 \\ 0 & 14.864 & 0 & 0 \\ 0 & 0 & 11.099 & 0 \\ 0 & 0 & 0 & 0 \end{bmatrix} \times 10^{-8} \frac{rad.m}{N}$

Now the product of the matrix [C][E] becomes:

$$[C][E] = \begin{bmatrix} 0.462 & 1.071 & 1.800 & 0 \\ 0.578 & 0.517 & 0.869 & 0 \\ 0.747 & 0.669 & 0.500 & 0 \\ 0 & 0 & 0 & 0 \end{bmatrix} \times \frac{10^{-6} rad.m^2}{N}$$

```
%MATLAB script for iteration convergence
clc;
C=[31.275 31.275 31.275 0; 37.53 12.067 12.067 0; 31.275 12.067 5.365 0; 0 0 0 0]*0.00000001
e=[0.278 0 0 0; 0 0.348 0 0; 0 0 0.45 0; 0 0 0 0.572]
```

```
w=[1.91 0 0 0; 0 3.54 0 0; 0 0 4.6 0; 0 0 0 2.494]
E=C*e*w
c=[2.78 0 0 0; 0 3.48 0 0; 0 0 4.5 0; 0 0 0 5.715]
cE=c*E
A=c*E
clc;
A=[0.462 1.071 1.800 0; 0.578 0.517 0.869 0; 0.747 0.669 0.500 0; 0 0 0 0]*0.000001;
n=size(A,1)
tol=0.00001;
err=100;
x=[1 1 1 1]'
x=ones(n,1)
k=0;
while(err>tol)
x1=A*x;
[val,pos]=max(abs(x1));
eigen_val=x1(pos);
x2=x1/eigen_val;
err=max(abs(x2-x));
x=x2;
eigen_vec=x;
k=k+1;
end
fprintf('Break the loop when it converges after %d iterations', k);
```

After ten iterations of the matrix$[C][E] = 2.3 \times 10^{-6} \frac{rad.m^2}{N}$. Substituting the dynamic pressure $q_d\ by\ \frac{1}{2}\rho v_{Dinf}^2$, $\rho =$ 1.225 $kg/m^3$and $\frac{dc_l}{d\alpha}$=5.5, we get the divergence speed of infinite wing becomes: $v_{Dinf} = 359.25\ ^m/_{sec}$. Similarly, the divergence speed for finite span correction with $\frac{dc_l}{d\alpha} = 3.93$ becomes: $v_{Df} = 425\ ^m/_{sec}$.

6. Result and Discussion

Divergence speed of the wing of a jet transport have been estimated under the following three different conditions:

a) Using strip theory without finite span correction.

b) Using strip theory with finite span correction.

c) A tentative Increment of the torsional stiffness of the wing by 20%.

It is seen that divergence speed is about 18.28% higher when the finite span correction is applied. This means that the method of analysis using strip theory without finite span correction is conservative since it yields divergence speed which is less than that of a three-dimensional wing.

To study the effect of torsional stiffness of the wig up on the divergence speed, a 20% increase in torsional stiffness is tentatively considered and the divergence speed is estimated using strip theory with finite span correction. It is found that divergence speed is increased by about 18.30% when the torsional stiffness is increased by 20%. This may be attributed to the fact that divergence speed of a wing is directly proportional to the torsional stiffness of a wing.

7. Conclusion

An attempt has been made in this work to study the divergence characteristics of the wing of a typical jet transport aircraft. Torsional influence coefficient matrix of four Multhopp's stations has been developed using the torsional stiffness data of the wing of a typical jet transport aircraft. Torsional influence coefficient can be used for estimating the torsional deflection of a wing subjected to pure torsion. This matrix, however, is developed to estimate the divergence speed of the wing, using matrix iteration technique. Elastic twist distribution, $\theta(y)$ and lift coefficient $c_l^e(y)$ are the unknown in the governing integral equation and the problem is thus statically indeterminate. Strip theory is employed to overcome this problem. The governing integral equation is solved numerically using matrix method. The divergence speed of the wing has been estimated using strip theory with and without finite span corrections. The effect of torsional stiffness of the wing upon torsional divergence speed has also been studied.

It is observed that torsional divergence speed is estimated on the basis of strip theory without finite span correction (two-dimensional wing) is about 18.28 percent lower than the divergence speed estimated on the basis of strip theory with finite span correction (three-dimensional wing). Two-dimensional torsional divergence analysis based on strip theory yields conservative torsional divergence speed. A tentative increase of 20 percent in torsional stiffness resulted in about 18.3 percent increase in torsional divergence speed of a three-dimensional wing. This shows that divergence speed of a wing is directly proportional to the square root of torsional stiffness. This corroborates the result obtained for a two-dimensional wing in ref [4]. The result of the study is mandatory to the design of high-performance modern airliners and useful to designers for static aeroelastic analysis of jet airplane wings.

Abbreviations

q_i = Generalized cooordinate.

C_{ij} = flexibility influence coefficient.

Q_i = Generalized forces.

U = Strain energy.

559 $T(y)$ = Torque at station y.

560 $t(y)$ = Applied torque per unit span.

561 q = Shear flow.

562 c. s. = Cloased section.

563 L = Length of the beam.

564 q_i = Generalized cooordinate.

565 G = Shear modulus.

566 $\vartheta(\lambda, s)$ = Shear flow distribution due to $T = 1$(Unit torque).

567 t = wing skin thickness.

568 J = torsional constant of the wing cross section.

569 λ, η, y = Stations along the wing span.

570 $C^{\theta\theta}$ = Torsional influenece coefficient.

571 $q_d = 1/2\,\rho v^2$ = Divergence dynamic pressure .

572 v_D = Divergence speed.

573 v_{D_f} = Divergence speed for finite wing.

574 $v_{D_{inf}}$ = Divergence speed for infinite wing.

575 c_i = local lift coefficient.

576 $C_{m_{a.c}}$ = Local moment coefficients about the aerodynamic center.

577 C = Wing chord.

578 C_i = Chord lenght at station i.

579 b = Wing semi − span.

580 a_o = Slope of the lift coefficient curve .

581 c_i = local lift coefficient.

582 N = Load factor normal to the wing surface.

583 d = distance between elastic axis and center of gravity.

584 e = Aerodynamic eccentricity.

585 θ = Angle of twist about elastic axis.

586 $\alpha(y) =$ Angle of attack.

587 $c_l^r(y) =$ local lift coefficient distribution resulting from rigid twist, $\alpha^r(y)$

588 $c_l^e(y) =$ local lift coefficient distribution resulting from elastic twist .

589 $\Theta =$ the linear operator on the lift distribution, cc_l

590 $L.E =$ Wing leading edge.

591 $T.E =$ Wing trailing edge.

592 $A.C =$ Aerodynamic center.

593 $E.A =$ Elastic axis.

594 $S.C =$ Shear center.

595 $2D =$ two dimentional.

596 $3D =$ three dimentional.

597 **Availability of data and materials**: The author declares that the data supporting the findings of this study are
598 available within the article.

599 **Competing interests:** This manuscript has not been submitted to, or under review at, any of another journal or
600 publication site; The author has no affiliation with any organization with a direct or indirect financial interest in the
601 subject matter discussed in the manuscript.

602 **Funding:** This research received no external funding.

603 **Authors' contributions:** The Author has involved in (a) literature reviewing, mathematical formulations and
604 numerical computations, analysis, and interpretation of the final findings; (b) drafting and writing the manuscript; and
605 (c) approval of the final work together with the decision to submit the article for publication.

606 **Acknowledgements:** The authors gratefully acknowledge and like to thank the reviewers of this paper for their
607 insightful comment. The author also wishes to thank the publishing organization, the ***Chinese Aerodynamics***
608 ***Research Society*** for the kind financial support provided to publish this paper.

609 **Authors' information**

610 Kirubeil Awoke Ferede.

611 Department of Mechanical Engineering, University of Gondar, Technology Institute Gondar, Ethiopia.

612 Researcher, Technology Transfer, and Community Engagement.

613 Mechanical Design Stream Chair Person.

614 Mobile Phone: +251922956733

615 Kb1981gc@gmail.com, Kiru1981gc@gmail.com

P.O. Box:196

www.uog.Edu.et

References

1. M. Xu, X. An, W. Kang, and G. Li (2020) Modern Computational Aeroelasticity. De Gruyter.
2. S. Heinze, J. R. Wright, and J. E. Cooper (2008) Introduction to aircraft aeroelasticity and loads, vol. 20. John Wiley & Sons.
3. S. Heinze (2007) “Aeroelastic concepts for flexible aircraft structures.” KTH.
4. R. L. Bisplinghoff, H. Ashley, and R. L. Halfman (2013) Aeroelasticity. Courier Corporation.
5. R. P. Goff (1998) “Airplane stability and control: A history of the technologies that made aviation possible,” Endeavour, vol. 22, no. 3, pp. 133–134, doi: 10.1016/s0160-9327(99)80022-2.
6. L. S. Rolls and F. H. Matteson (1952) “Wing Load Distribution on a Swept Wing Airplane in Flight at Mach Numbers up to 1.11, and Comparison with Theory,” .
7. H. Multhopp (1950) “Methods for calculating the lift distribution of wings subsonic lifting-surface theory,”.
8. I. H. Abbott and A. E. Von Doenhoff (2012)Theory of wing sections: including a summary of airfoil data. Courier Corporation.
9. S. PINES (1949) “A Unit Solution for the Load Distribution of a Nonrigid Wing by Matrix Methods,” J. Aeronaut. Sci., vol. 16, no. 8, pp. 470–476, doi: 10.2514/8.11835.
10. H. R. Cox and A. Pugsley (1933) Stability of static equilibrium of elastic and aerodynamic actions on a wing. HM Stationery Office.
11. W. R. Sears (1948) “A new treatment of the lifting-line wing theory, with applications to rigid and elastic wings,” Q. Appl. Math., vol. 6, no. 3, pp. 239–255.
12. A. STRIZ and Y. LOO (1993) “Application of differential quadrature to the analysis of static aeroelastic phenomena,” in 34th Structures, Structural Dynamics and Materials Conference, p. 1505.
13. Y. C. Fung (2008) An introduction to the theory of aeroelasticity. Courier Dover Publications.
14. O. Stodieck, J. E. Cooper, P. M. Weaver, and P. Kealy (2017) “Aeroelastic tailoring of a representative wing box using tow-steered composites,” AIAA J., vol. 55, no. 4, pp. 1425–1439, doi: 10.2514/1.J055364.
15. J. P. Fielding (1999) Introduction to Aircraft Design.

16. S. Qiao, J. Jiao, Y. Ni, H. Chen, and X. Liu (2021) “Effect of Stiffness on Flutter of Composite Wings with High Aspect Ratio,” Math. Probl. Eng., vol. 2021, doi: 10.1155/2021/6683032.
17. S. A. Fazelzadeh, M. Rezaei, and A. Mazidi (2020) “Aeroelastic analysis of swept pre-twisted wings,” J. Fluids Struct., vol. 95, p. 103001, doi: 10.1016/j.jfluidstructs.2020.103001.
18. A. R. Torabi, S. Shams, M. Fatehi Narab, and M. A. Atashgah (2021) “Delamination effects on the unsteady aero-elastic behavior of composite wing by modal analysis,” J. Vib. Control, p. 10775463211019212.
19. S. Townsend, R. Picelli, B. Stanford, and H. A. Kim (2018) “Structural optimization of platelike aircraft wings under flutter and divergence constraints,” AIAA J., vol. 56, no. 8, pp. 3307–3319, doi: 10.2514/1.J056748.
20. X. Rongrong, Y. Zhengyin, Y. Kun, and W. Gang (2019) “Composite material structure optimization design and aeroelastic analysis on forward swept wing,” Proc. Inst. Mech. Eng. Part G J. Aerosp. Eng., vol. 233, no. 13, pp. 4679–4695, doi: 10.1177/0954410018807810.
21. M. Rasool and M. K. Singha (2020) “Aeroelastic analysis of pre-stressed variable stiffness composite panels,” JVC/Journal Vib. Control, vol. 26, no. 9–10, pp. 724–734, doi: 10.1177/1077546319889865.
22. M. Ashktorab, F. Taheri-Behrooz, and Z. Zamani (2021) “Flutter analysis of a sandwich composite beam using an analytical method,” J. Sandw. Struct. Mater., vol. 23, no. 8, pp. 3814–3835, doi: 10.1177/1099636220948417.
23. M. Mahran, H. Negmb, K. Maalawic, and A. El-Sabbaghd (2015) “Aero-elastic analysis of composite plate swept wings using the finite element method,” Lisbon, Port..
24. M. K. Abbas, H. M. Negm, and M. A. Elshafei (2013) “Flutter and divergence characteristics of composite plate wing,” in International Conference on Aerospace Sciences and Aviation Technology, vol. 15, no. AEROSPACE SCIENCES & AVIATION TECHNOLOGY, ASAT-15–May 28-30, 2013, pp. 1–21.
25. M. Serry and A. Tuffaha (2018) “Static stability analysis of a thin plate with a fixed trailing edge in axial subsonic flow: possio integral equation approach,” Appl. Math. Model., vol. 63, pp. 644–659.
26. M. Yu and C. Hwu (2007) “Aeroelastic divergence and free vibration of tapered composite wings,” ICCM Int. Conf. Compos. Mater., pp. 1–7.
27. T. Ueda (2005) “Aeroelastic analysis considering structural uncertainty,” Aviation, vol. 9, no. 1, pp. 3–7.

672 28. H. T. K. Dung and N. P. Khanh (2020) “Research on Aeroelasticity Phenomenon in Aeronautical
673 Engineering,” in Aerodynamics, IntechOpen.
674 29. J. A. Haught and J. A. Haught (2020) “Aeroelasticity of Composite Plate Wings using HSDT and Higher-
675 Order FEM Aeroelasticity of Composite Plate Wings using HSDT and Higher-Order FEM,”.
676 30. J. Flis, M. Augustyn, and A. Muc (2020) “Divergence and Flutter of Multilayered Laminated Structures,” J.
677 Phys. Conf. Ser., vol. 1603, no. 1, doi: 10.1088/1742-6596/1603/1/012006.
678 31. W. P. Rodden (1959) “Aerodynamic influence coefficients from strip theory,” J. Aerosp. Sci., vol. 26, no.
679 12, pp. 833–834.
680 32. C. C. Xie, Y. Liu, and C. Yang (2012) “Theoretic analysis and experiment on aeroelasticity of very flexible
681 wing,” Sci. China Technol. Sci., vol. 55, no. 9, pp. 2489–2500, doi: 10.1007/s11431-012-4941-3.
682 33. T. H. G. Megson, (2016) Aircraft structures for engineering students. Butterworth-Heinemann.
683 34. Z. Qin, P. Marzocca, and L. Librescu (2002) “Aeroelastic instability and response of advanced aircraft
684 wings at subsonic flight speeds,” Aerosp. Sci. Technol., vol. 6, no. 3, pp. 195–208.
685 35. J. S. Przemieniecki (1985) Theory of matrix structural analysis. Courier Corporation.
686 36. H. Multhopp (1950) “Methods for Calculating the Lift Distribution of Wings (Subsonic Lifting-Surface
687 Theory).,” Aeronaut. Res. Counc., vol. 2884, no. 2884, pp. 1–96,
688 http://repository.tudelft.nl/view/aereports/uuid:06d93da1-0801-4c99-80ca-06fac0b0c11d/.
689 37. B. K. Donaldson (2008) Analysis of Aircraft Structures: An Introduction (Cambridge Aerospace Series).
690 38. D. E. Bossert, S. L. Morris, W. F. Hallgren, and T. R. Yechout (2003) Introduction to aircraft flight
691 mechanics: Performance, static stability, dynamic stability, and classical feedback control. American
692 Institute of Aeronautics and Astronautics.

693